Supplement of Biogeosciences, 17, 2647–2656, 2020
https://doi.org/10.5194/bg-17-2647-2020-supplement

Biogeosciences Open Access EGU

Supplement of

Large-scale biospheric drought response intensifies linearly with drought duration in arid regions

René Orth et al.

Correspondence to: René Orth (rene.orth@bgc-jena.mpg.de)

Supporting Information for

Large-scale biospheric drought response intensifies linearly with drought duration in arid areas

Rene Orth, Georgia Destouni, Martin Jung, Markus Reichstein

Methods

In order to enable joint analyses we aggregate all employed datasets to the lowest of their individual spatial and temporal resolutions, which are 0.5°x0.5° and half-monthly, respectively. For this purpose, for every 0.5°x0.5° grid cell, we compute the mean across all sub-grid cells. Half-monthly temporal data is obtained by averaging all (sub-)daily data across the first 15 days of each month, and across the remaining days. This is done only if values are available for at least 6 days out of the half-monthly period. In the case of the 8-daily GPP and ET data we infer half-monthly estimates by computing weighted means of the 8-day periods within a half-monthly interval; the weights are thereby determined from the amount of days of each 8-day period that are within the considered half-monthly interval.

All analyses are restricted to time periods when all concerned data products are available.

Datasets

A) Drought forcing datasets

A1) Soil Moisture:

We employ the gridded surface soil moisture dataset from the European Space Agency's (ESA) Climate Change Initiative (CCI), version 4.4 (http://www.esa-soilmoisture-cci.org, accessed on 2 August 2018). Therefrom, we use the combined product which is derived with observations from active and passive satellites *(14)*. This is a global product which covers the time period 1978-2016. The native spatial and temporal resolutions are 0.25°x0.25° and 1 day, respectively.

A2) Precipitation:

Gridded precipitation is obtained from the ERA-Interim reanalysis dataset *(15)*. The data is available between 1979-2015, and the spatial and temporal resolutions are 0.5°x0.5° and 1 day, respectively.

A3) Net radiation:

We use satellite-derived net radiation data from (i) the Surface Radiation Budget (SRB) dataset, version 3.1 (https://gewex-srb.larc.nasa.gov, accessed on 6 April 2018), and (ii) the Clouds and the Earth's Radiant Energy System (CERES) dataset, version 4 (https://ceres.larc.nasa.gov/, accessed on 6 April 2018). Both datasets are global, and have a spatial resolution of 1°x1°. The SRB dataset has a temporal resolution of 3 hours, while the CERES product provides daily data. While the SRB dataset extents between 1983-2007, the CERES data are available between 2000-2016. In order to obtain a consistent time series we merge both products by scaling the SRB data to the mean and standard deviation of the CERES data from the respective grid cell using data from the overlapping time period 2000-2007 (as done in *32*).

B) Vegetation datasets

B1) Gross Primary Productivity (GPP) and evapotranspiration (ET):

We employ GPP and ET data from the FluxCom dataset *(16)*. Therefrom we use the RS product. It is derived by upscaling site-level observations in conjunction with satellite data using multiple machine learning methods. This global product spans between 2001-2015. Its spatial and temporal resolutions are 0.083°x0.083° and 8 days, respectively.

B2) Normalized Differential Vegetation Index (NDVI):

Gridded NDVI data are obtained from the Global Inventory Modeling and Mapping Studies (GIMMS) product, version 3g *(17)*. This product is derived from satellite observations. It is a global dataset which covers the time period 1982-2015. Its spatial and temporal resolutions are 0.083°x0.083° and half-monthly, respectively.

B3) Agricultural yields:

We use information on agricultural yields from the EUROSTAT database which summarizes crop yield statistics for various European countries (http://appsso.eurostat.ec.europa.eu/nui/, accessed on 6 April 2018). In particular we use data on 5 major crops: “cereals (excluding rice)”, “wheat (including spelt)”, “grain maize and corn-cob-mix”, “potatoes (including early potatoes and seed potatoes)”, and “sugar beet (excluding seed)”. The data are available between 1950-2015, even though only few countries reported data earlier than 1990. In order to isolate climate-induced variations in crop yields from anthropogenic effects (e.g. technical progress), we removed the long-term trend from each crop yield time series; this trend is determined with fitted cubic smoothing splines (as in *36*).

C) Irrigation data

Irrigation data is also employed from the EUROSTAT database which provides corresponding statistics for various European countries (http://appsso.eurostat.ec.europa.eu/nui/, accessed on 6 April 2018). The data are available for the years 2005, 2007, 2010, 2013. In order to infer the relative importance of irrigation in each country we compute the ratio of the mean area “irrigated at least once a year : Total (excl kitchen gardens and area under glass)” across the available years, and the mean “utilised agricultural area” as also determined from the available years.

D) Land cover data

The fraction of agricultural area within a grid cell is determined from the MODIS (Moderate Resolution Imaging Spectroradiometer) product MCD12Q1. Thereby, we consider cropland and mosaics between cropland and natural vegetation. This global dataset is invariant in time, and has a spatial resolution of 0.5°x0.5°.

Additional references not contained in main manuscript

41. Zscheischler, J., Orth, R., Seneviratne S. I., European crop yields predicted by bivariate return periods of temperature and precipitation, *Biogeosciences* **14**, 3309-3320 (2017).

Supplementary Table 1: Individual models used in Figure 4, and respective results.

Model	Drought-int. transpiration. ano. at 5 months (in StDev for the 5 considered aridity classes)	Drought-int. transpiration ano. at 10 months (in StDev for the 5 considered aridity classes)
GLEAM	-3/-13/-38/-104/-77	-/-72/-48/-120/-91
PCR-GLOBWB	-47/-78/-47/-77/-74	-/-63/-49/-80/-96
W3RA	-62/-95/-102/-112/-95	-/-80/-85/-109/-91
HTESSEL-CaMa	-60/-84/-88/-103/-73	-/-45/-48/-94/-52
LISFLOOD	-10/-35/-45/-55/-47	-18/-53/-44/-64/-73
SURFEX-TRIP	10/-24/-56/-90/-66	-/-26/-25/-76/-72
JULES	-31/-76/-80/-101/-71	-/-65/-79/-96/-67

Supplementary Table 2: Individual models used in Figure S3, and respective results.

Model	Drought-int. transpiration ano. at 5 months (in StDev for the 5 considered aridity classes)	Drought-int. transpiration ano. at 10 months (in StDev for the 5 considered aridity classes)
GLEAM	17/4/-21/-73/-59	-/-55/-42/-104/-96
PCR-GLOBWB	-22/-44/-55/-75/-65	-119/-80/-63/-98/-92
W3RA	-43/-82/-81/-89/-74	-111/-91/-91/-113/-92
HTESSEL-CaMa	-9/-36/-30/-32/-30	-8/-55/-61/-90/-48
LISFLOOD	-10/-34/-45/-55/-46	-20/-55/-44/-65/-72
SURFEX-TRIP	-8/-14/-40/-60/-53	-22/-29/-58/-88/-70
JULES	-16/-29/-34/-39/-27	-21/-58/-55/-78/-50
CABLE	8/-3/-24/-30/-30	-29/-65/-53/-73/-51
ISAM	13/-5/-22/-23/-20	-15/-12/-25/-86/-72
JULES	27/-40/-30/-55/-23	-75/-80/-96/-104/-70
LPJ	-52/-23/-32/-51/-58	-51/-25/-22/-59/-83
LPJ-GUESS	77/29/-9/-31/-43	13/-14/-30/-66/-62
ORCHIDEE	11/-44/-38/-60/-52	-69/-94/-71/-96/-87
VEGAS	11/7/13/-17/-49	-34/-50/-28/-92/-147
VISIT	-12/-38/-41/-55/-77	-18/-125/-112/-107/-129

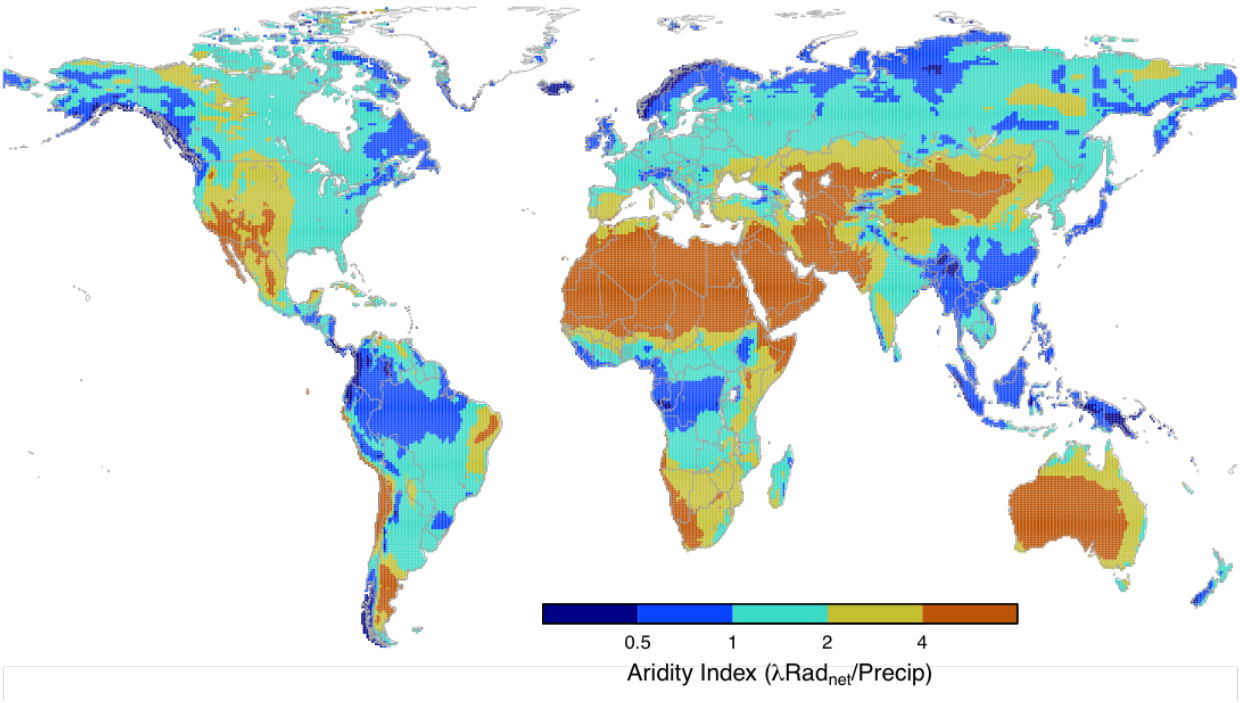

Supplementary Figure 1: Map of aridity indices.

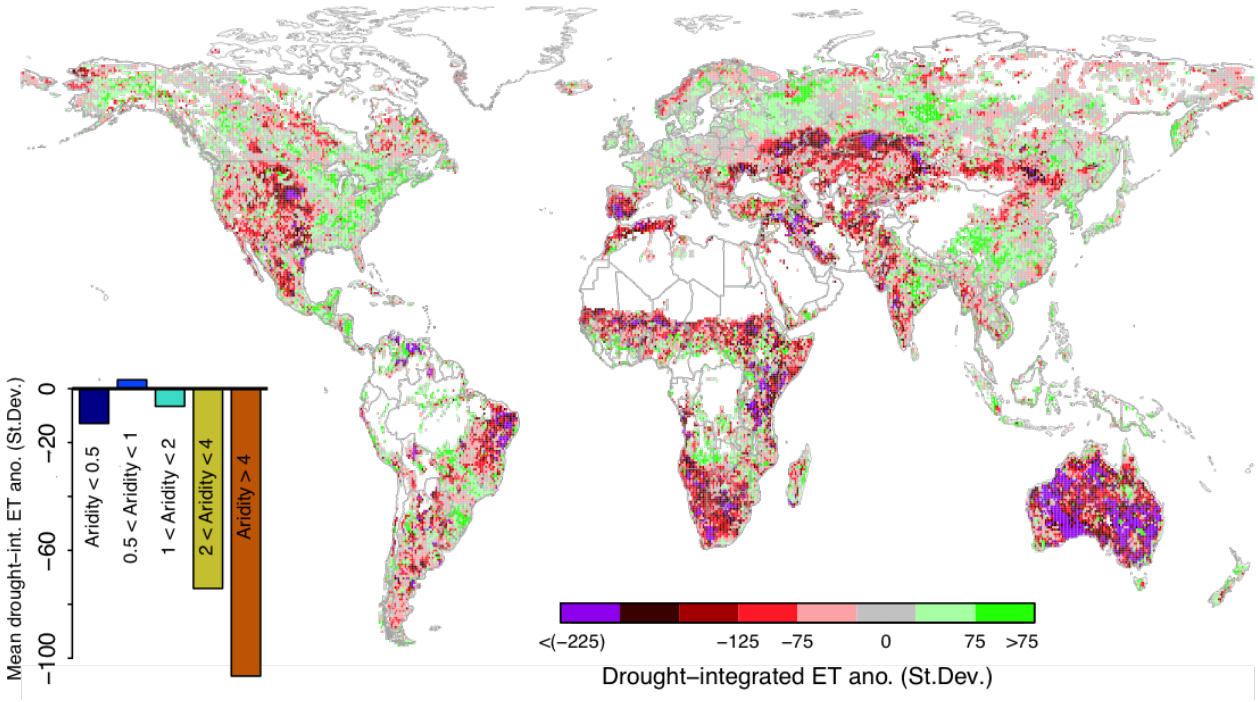

Supplementary Figure 2: Same as in Figure 1, but computed with ET data.

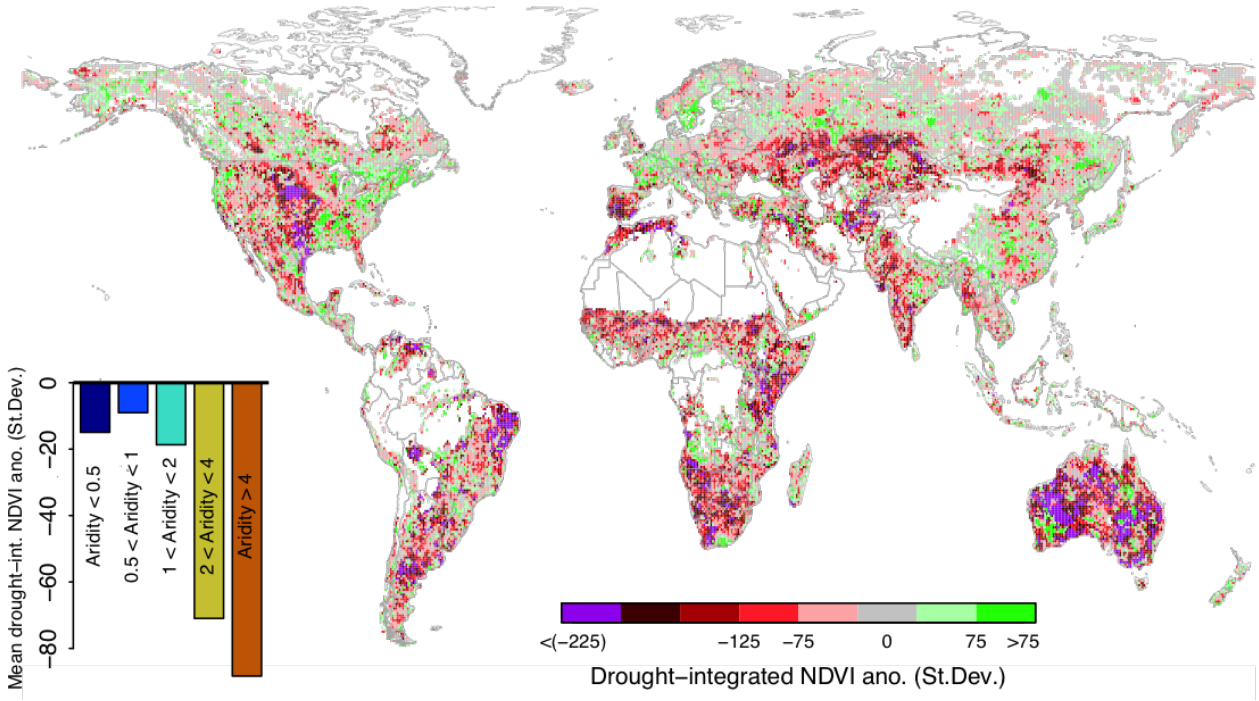

Supplementary Figure 3: Same as in Figure 1, but computed with NDVI data.

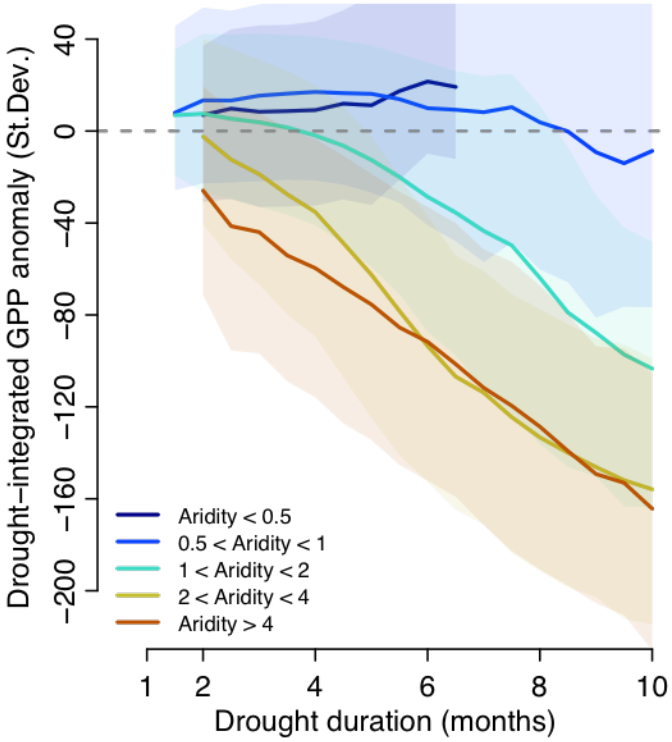

Supplementary Figure 4: Similar to Figure 3, but with strongest grid-cell droughts determined through the longest period of consecutive negative soil moisture anomalies during the growing season.

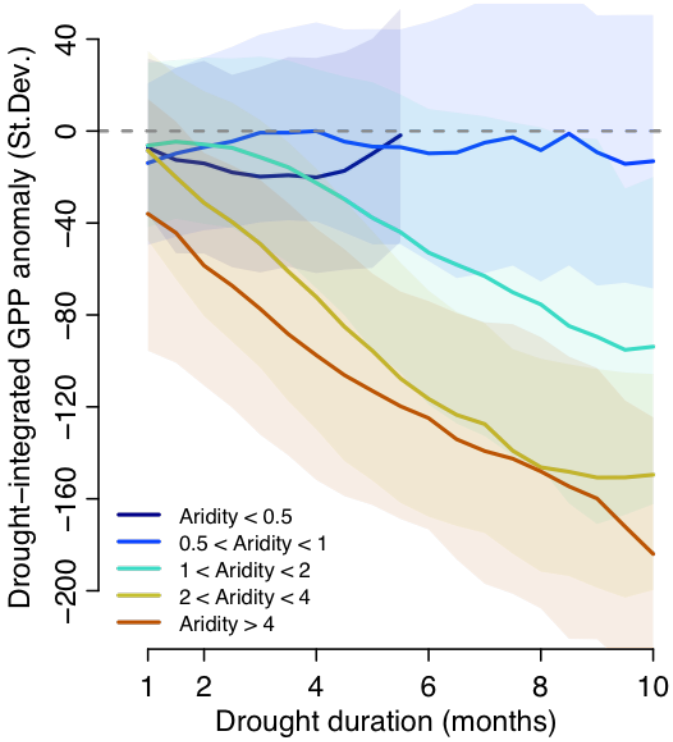

Supplementary Figure 5: Similar to Figure 3, but with 6-months time window for determining the drought-integrated GPP anomaly.

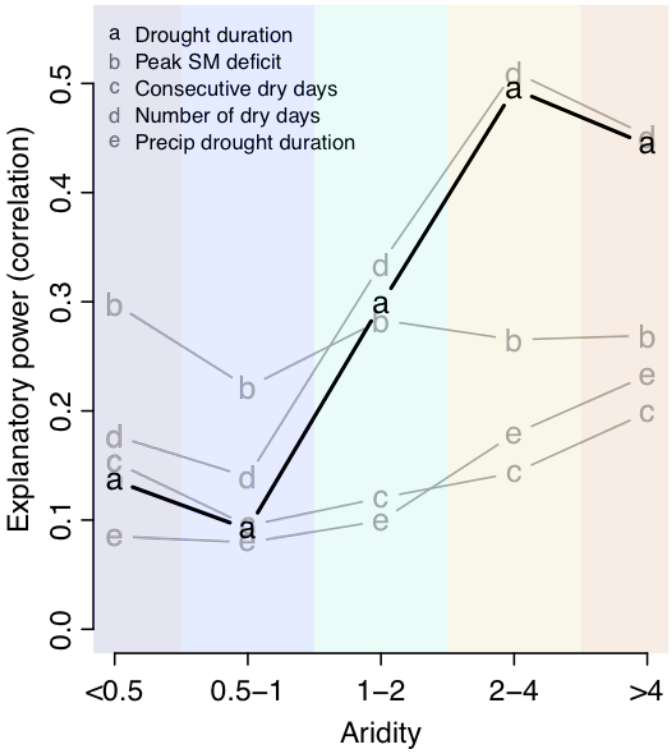

Supplementary Figure 6: Fraction of variance in drought-integrated GPP anomalies explained by drought duration relationships (as displayed in Figure 3), and alternative controls.

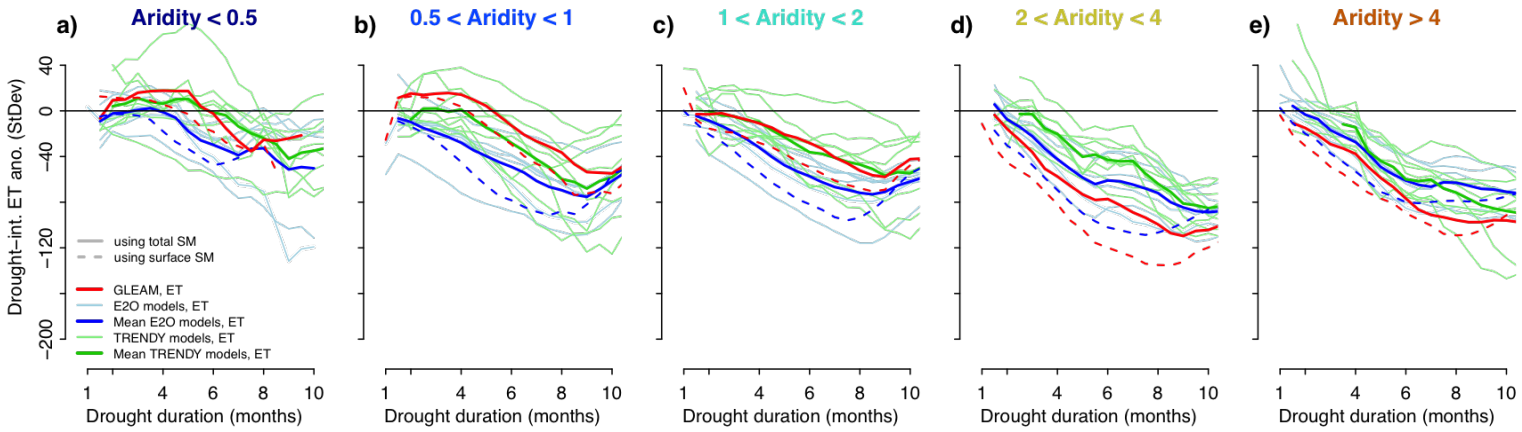

Supplementary Figure 7: Similar to Figure 4, but for deep soil moisture (except the observational reference which is only displayed for comparison, black line). Because of availability of deep soil moisture only, TRENDY models are considered here (green lines) in addition to the models used in Figure 4.